PROCEEDINGS A

rspa.royalsocietypublishing.org

Research

Article submitted to journal

Subject Areas:
Applied mathematics,
Electromagnetism,
Partial differential equations

Keywords:
Power series, Homogenization,
Sub-wavelength resonance,
Maxwell's equations, Metmaterial
crystals

Author for correspondence:
Abiti Adili
e-mail: abiti_adili@uml.edu

THE ROYAL SOCIETY
PUBLISHING

Controlling the Dispersion of Metamaterials in 3-d

Abiti Adili[1,5], Yue Chen[2,5], Robert Lipton[3,5] and Shawn Walker[4,5]

[1]Department of Mathematical Sciences, University of Massachusetts Lowell, Lowell, MA, 01854
[2]Department of Mathematics, Auburn University at Montgomery, Montgomery, AL 36117
[3,4]Department of Mathematics, Louisiana State University, Baton Rouge, LA, 70803
[5] ORCID AA, 0000-0001-6451-6960; YC, 0000-0003-1724-5197; RL, 0000-0002-1382-3204; SW, 0000-0002-8027-5789

We provide a platform to examine the effect of inclusion geometry on three dimensional metamaterial crystals to tune frequency dependent effective properties for control of leading order dispersive behaviour. The crystal is nonmagnetic and made from all dielectric components. The design provides novel dispersive properties using subwavelength resonances controlled by the geometry of the media. We numerically calculate the effective tensors of the metamaterial to identify frequency intervals where the metamaterial exhibits band gaps as well as intervals of normal dispersion and double negative dispersion. The frequency intervals can be explicitly controlled by adjusting the geometry and placement of the dielectric inclusions within the period cell of the crystal.

1. Introduction and Problem Setup

(a) Introduction

Metamaterials exhibit novel properties not found in nature. These properties are generated by periodically patterned composite material crystals. When the period of the crystal is less than the wavelength of incident radiation, interesting interactions occur between the material and the electromagnetic waves. This provides the opportunity for manipulation of structural geometry to obtain novel dispersive properties. One such property is exhibited by the double negative metamaterial which has frequency dependent negative effective magnetic

permeability and negative effective dielectric permittivity. Metamaterials with double negative effective properties have wide range of applications ranging from biomedical imaging to optical litho-graphy and data storage. In 1968, the novel properties of materials were studied under the assumption of negative dielectric constant and negative magnetic permeability [1]. The double negative effective properties of periodic array of non-magnetic metallic split-ring resonators at microwave frequency were studied in [2]. The double negative properties of metamaterials made from arrays of metallic posts and split ring resonators were experimentally demonstrated in [3]. Double negative properties of materials were obtained for metallic resonators with different geometric structures in [4–9]. Negative refractive properties of metamaterials obtained by employing dielectric material with large permittivity were studied in [10–12].

The appearance of double negative properties of metamaterials made from high dielectric core with plasmonic coating at optical frequencies was explored in [13–15]. Metamaterial crystals with double negative effective properties were obtained using periodic array of unit cells consisting of two different inclusions in [16,17]. Negative bulk dielectric permeability at infrared and optical frequencies using special configurations of plasmonic nanoparticles was studied in [18,19].

The dispersion relation and convergent power series representation for a propagating Bloch wave in a periodic media with a single high contrast inclusion were obtained in [20–22]. The leading order terms give the effective dispersion relation of the metamaterial while the higher order terms give the corrections necessary for the diffraction due to inclusions of finite size. In the optical frequency regime, convergent power series solutions recovering dispersion relations were derived for all dielectric constituents that deliver double negative dispersive properties for TE modes propagating transverse to prismatic rods [17]. For these configurations the direction of power flow is opposite to phase velocity. Their frequency dependent refractive properties were subsequently engineered in the time domain for controlling the direction of signals [23]. A setting for which the appearance of artificial magnetism for describing scattering problems for 3D metamaterials using high dielectric constant inclusions was introduced and rigorously established in [24]. For 3D metallic split ring geometries the rigorous proof of effective magnetic permeability was recently given in [25]. Recently, the rigorous mathematical realization of double negative metallic media using two scale expansions for microwave frequencies were obtained in [26].

This paper analyzes metamaterial crystals constructed using all dielectric materials in the near infrared-optical regime. Our choice of dielectric constituents is motivated by the work of [17]. The novelty of this work is that we focus on fully 3D materials and the results are directly obtained from Maxwell's equations using power series expansions of the electromagnetic fields. The wavelength of light propagating through the periodic crystal is λ and the period of the crystal is d. For metamaterials the crystal is sub-wavelength, i.e., the period of the structure is below the wavelength of operation, so $2\pi d/\lambda < 1$. We treat a non-magnetic host dielectric M impregnated with an infinite periodic array of non-magnetic inclusions with different dielectric properties. Inside any period the host material contains two types of non-magnetic included phases: one with a high dielectric constant denoted by R and the other featuring a frequency-dependent dielectric constant denoted by P. The 3D period cube containing distinct inclusions of P and R is shown in Figure 1 and a coated sphere geometry with core R coated with P is shown in Figure 2. The leading order behavior of the electromagnetic field inside a metamaterial made from these configurations are propagating plane waves with polarization given by averaged electric and magnetic fields. The plane waves can propagate across frequency bands determined explicitly to leading order by a dispersion relation given in terms of frequency dependent effective magnetic permeability and permittivity. The averaged electric field is the usual average of the electric field over the period cell, however the averaged H field is based on a geometric average over the period introduced in [24] for periodic sub-wavelength high dielectric materials associated with artificial magnetization, see (2.8) and (2.9) of section (b). The frequency dependent effective dielectric permittivity and magnetic permeability are described by two types of subwavelength resonances: a plasmon resonance generating frequency dependent positive or negative effective

dielectric properties and an artificial magnetic resonance generating a frequency dependent effective magnetic permeability, see section (c). The plasomnic response of the metamaterial is due to the frequency dependence of the dielectric inclusion exciting a structural electric resonance of the electromagnetic crystal at certain frequencies. The structural resonance was calculated through generalized electrostatic resonances for periodic crystals [16,17,27]. This approach is motivated by the seminal work of [28,29] that introduces similar resonances to obtain bounds on frequency independent effective transport properties. For dilute suspensions such resonances can be found in [30]. The magnetic resonances were mathematically identified and explained in the three dimensional context in [24], see also [31,32]. Here we show how to employ these two resonances to rationally design double negative materials. We numerically calculate the effective properties for metamaterial crystals made from coated sphere geometries and identify frequency intervals in the optical regime where the metamaterial exhibits double negative behavior. Here the term double negative refers to simultaneously negative effective magnetic permeability and dielectric permittivity, implying that the propagation of energy is opposite to the direction of phase velocity. This is demonstrated in section (d).

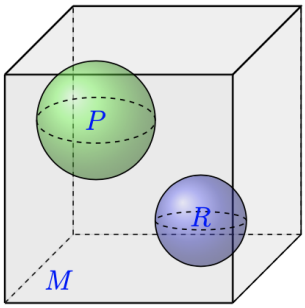

Figure 1: Period Cell

(b) Problem Setup

The Maxwell system takes the form

$$\begin{aligned} \nabla \times E &= -\mu_d \frac{\partial H}{\partial t}, \\ \nabla \cdot (\varepsilon_d E) &= 0, \\ \nabla \times H &= \varepsilon_d \frac{\partial E}{\partial t}, \\ \nabla \cdot H &= 0. \end{aligned} \tag{1.1}$$

Here E denotes the electric field and $H = B/\mu_0$ where B is the magnetic field. The host and inclusions are non-magnetic and $\mu_d := \mu_0$ everywhere in the crystal where μ_0 is the free space value.

We express Maxwell's equations in terms of relative dielectric permittivity and magnetic permeability. And the dielectric constant $\varepsilon_d(\boldsymbol{x})$ of the metamaterial crystal of period length d with period cell $Y^d = (0,d)^3$ is given by $\varepsilon_d = \epsilon_0 \varepsilon^d_{rel}$ where ϵ_0 is the dielectric constant in free space and the relative dielectric permittivity

$$\varepsilon^d_{rel} = \begin{cases} \varepsilon_{p,rel}(\omega) = 1 - \frac{\omega_p^2}{\omega^2} & \text{in } P, \\ \dfrac{\varepsilon_{r,rel}}{d^2} & \text{in } R, \\ 1 & \text{in } M. \end{cases} \tag{1.2}$$

Here $\varepsilon_{p,rel}$ and $\varepsilon_{r,rel}$ represent the dielectric constants of the inclusions P and R respectively, and unity is the relative dielectric constant for free space. The material characterized by $\varepsilon_{p,rel}$ is frequency dependent like gold or aluminum for near infrared and optical frequencies. To illustrate the idea, $\varepsilon_{p,rel}$ is represented by a Drude model without damping where ω_p is the plasma frequency. The material inside inclusion R is a frequency independent dielectric material.

We consider periodically modulated waves propagating through the crystal,

$$E(\boldsymbol{x},t) = E(\boldsymbol{x})e^{(ik\hat{k}\cdot\boldsymbol{x}-i\omega t)} \quad \text{and} \quad H(\boldsymbol{x},t) = H(\boldsymbol{x})e^{(ik\hat{k}\cdot\boldsymbol{x}-i\omega t)}, \tag{1.3}$$

where $E(\boldsymbol{x})$ and $H(\boldsymbol{x})$ are periodic, $\hat{k}$ is the direction of wave propagation and $|\hat{k}| = 1$, k is the wave number, and ω is the frequency. Writing

$$\mathcal{E}(\boldsymbol{x}) = E(\boldsymbol{x})e^{ik\hat{k}\cdot\boldsymbol{x}} \quad \text{and} \quad \mathcal{H}(\boldsymbol{x}) = H(\boldsymbol{x})e^{ik\hat{k}\cdot\boldsymbol{x}},$$

and rescaling $\boldsymbol{y} = \boldsymbol{x}/d$, we have the problem posed in the unit cell $Y = (0,1)^3$ given by

$$\begin{aligned} \nabla\times\mathcal{E} &= id\omega\mu_0\mathcal{H}, & [\mathcal{H}] &= 0,\\ \nabla\times\mathcal{H} &= -id\omega\varepsilon_0\varepsilon_{rel}^d\mathcal{E}, & [n\times\mathcal{E}] &= 0,\\ \nabla\cdot\varepsilon_0\varepsilon_{rel}^d\mathcal{E} &= 0, & [n\cdot\varepsilon_0\varepsilon_{rel}^d\mathcal{E}] &= 0,\\ \nabla\cdot\mathcal{H} &= 0, \end{aligned} \tag{1.4}$$

where the notation $[\cdot]$ indicates transmission conditions across interfaces between materials.

In this paper power series expansion of the waves in the small parameter $\eta = dk = 2\pi d/\lambda$ is used to investigate dispersion associated with sub-wavelength crystals. We expand the electric field, magnetic field and non-dimensional square frequency as

$$\begin{aligned} \mathcal{E}(\boldsymbol{y}) &= \boldsymbol{e_0}(\boldsymbol{y})e^{i\eta\hat{k}\cdot\boldsymbol{y}} + \boldsymbol{e_1}(\boldsymbol{y})\eta e^{i\eta\hat{k}\cdot\boldsymbol{y}} + \boldsymbol{e_2}(\boldsymbol{y})\eta^2 e^{i\eta\hat{k}\cdot\boldsymbol{y}} + \cdots,\\ \mathcal{H}(\boldsymbol{y}) &= \boldsymbol{h_0}(\boldsymbol{y})e^{i\eta\hat{k}\cdot\boldsymbol{y}} + \boldsymbol{h_1}(\boldsymbol{y})\eta e^{i\eta\hat{k}\cdot\boldsymbol{y}} + \boldsymbol{h_2}(\boldsymbol{y})\eta^2 e^{i\eta\hat{k}\cdot\boldsymbol{y}} + \cdots,\\ \omega &= \omega_0 + \omega_1\eta + \omega_2\eta^2 + \cdots, \end{aligned}$$

where $\boldsymbol{e_0}, \boldsymbol{e_1}, \ldots$ and $\boldsymbol{h_0}, \boldsymbol{h_1}, \ldots$ are periodic. The expansions are substituted into (1.4) and the leading order terms $\boldsymbol{e_0}$, $\boldsymbol{h_0}$ together with the leading order dispersion relation relating ω_0 to k are seen to describe plane wave propagation inside the metamaterial, they give the leading order behavior for propagating electromagnetic waves inside the subwavelength medium for $2\pi d/\lambda < 1$.

2. Main Results

(a) Characterization of Leading Order Terms

The asymptotic analysis (see sections (b) and (e)) shows that the leading order terms $\boldsymbol{e}_0$ and $\boldsymbol{h}_0$ are characterized by solutions to quasi-static electromagnetic problems that can be written in terms of electrostatic and magnetostatic resonances.

Theorem 2.1. *The leading order H field, $\boldsymbol{h_0}$ is continuous and divergence free in Y. Moreover there is a periodic potential w and constant vector $\mathbf{c}$ such that $\boldsymbol{h}_0 = \nabla w + \mathbf{c}$ on $Y \setminus R$ with $\Delta w = 0$ there. Inside R, the quasistatic magnetic field $\boldsymbol{h}_0$ solves the Helmholtz equation*

$$\nabla\times\nabla\times\boldsymbol{h_0} = \xi_0\boldsymbol{h_0} \qquad \text{in } R, \tag{2.1}$$

where $\xi_0 = \epsilon_{r,rel}\,\omega_0^2/c^2$.

The effective magnetic activity is determined by the volume average of the leading order term $\boldsymbol{h}_0$. This is described with the aid of the geometric average $\oint \boldsymbol{h}_0$ of $\boldsymbol{h}_0$. To describe the geometric average consider a smooth vector field $\boldsymbol{v}$ defined on Y/R and periodic on the boundary of Y and introduce

$$\int_{\Gamma_{k,\boldsymbol{x}}} \boldsymbol{v} \cdot \tilde{\mathbf{e}}^k \, d\ell$$

with $\Gamma_{k,\boldsymbol{x}}$ being a curve connecting two points $\boldsymbol{x}$ and $\boldsymbol{x} + \tilde{\mathbf{e}}^k$ on opposite faces of the unit cube Y and arclength element $d\ell$. Here $\Gamma_{k,\boldsymbol{x}}$ can be any such curve lying outside of R. The geometric average $\oint \boldsymbol{v}$ exists if

$$\left(\oint \boldsymbol{v} \right) \cdot \tilde{\mathbf{e}}^k := \int_{\Gamma_{k,\boldsymbol{x}}} \boldsymbol{v} \cdot \tilde{\mathbf{e}}^k \, d\ell$$

is a unique constant vector independent of the choice of $\Gamma_{k,\boldsymbol{x}}$, $k = 1, 2, 3$. This is always the case when $\nabla \times \boldsymbol{v} = 0$ in $Y \setminus R$, see [31]. When $\nabla \times \boldsymbol{v} = 0$ in Y then $\oint \boldsymbol{v} = \int_Y \boldsymbol{v}$.

For $\boldsymbol{h}_0$ one has that

Corollary 2.1. *The geometric average of $\boldsymbol{h}_0$ is $\mathbf{c}$, where the constant vector $\mathbf{c}$ is defined in Theorem 2.1.*

The effective magnetic permeability [24,31,32] is defined to be the tensor $\boldsymbol{\mu}_{eff} = \boldsymbol{\mu}_{eff}(\omega_0)$ relating the volume average to the geometric average of the $\boldsymbol{h}_0$ field given by

$$\boldsymbol{\mu}_{eff} \left(\oint \boldsymbol{h_0} \right) = \int_Y \boldsymbol{h_0}(\boldsymbol{y}) d\boldsymbol{y}. \tag{2.2}$$

The explicit formula for $\boldsymbol{\mu}_{eff}$ is given in Theorem 2.6 and is constructed in Section (e).

The $\boldsymbol{e}_0$ field is the quasi-static electric field inside a periodic composite. We can write $\boldsymbol{e}_0$ as the sum of a potential gradient $\nabla\chi$ and a constant vector $\tilde{\mathbf{e}}$ where χ is periodic on Y. We set

$$a_p(\boldsymbol{y}) = \begin{cases} 1 & \boldsymbol{y} \in M \\ \varepsilon_{p,rel}(\omega_0) & \boldsymbol{y} \in P \end{cases} \tag{2.3}$$

and we have

Theorem 2.2. *The leading order term $\boldsymbol{e_0}$ satisfies*

$$\begin{aligned} &\nabla \times \boldsymbol{e_0} = 0 && \text{in } Y, \\ &\boldsymbol{e_0} = \nabla\chi + \tilde{\mathbf{e}} && \text{in } Y, \\ &\boldsymbol{e_0} = 0 && \text{in } R, \end{aligned} \tag{2.4}$$

with $\tilde{\mathbf{e}} = \int_Y \boldsymbol{e_0} \, d\boldsymbol{y}$ and the potential χ satisfies

$$\begin{aligned} &\nabla \cdot (a_p(\nabla\chi + \tilde{\mathbf{e}})) = 0 \quad \text{in } M \cup P, \\ &n \cdot \varepsilon_{p,rel}(\omega_0)(\nabla\chi + \tilde{\mathbf{e}})\big|_{\partial P^-} = n \cdot (\nabla\chi + \tilde{\mathbf{e}})\big|_{\partial P^+}, \end{aligned} \tag{2.5}$$

with

$$\chi + \tilde{\mathbf{e}} \cdot \boldsymbol{x} = 0 \text{ in } R, \tag{2.6}$$

where $\big|_{\partial P^-}$ and $\big|_{\partial P^+}$ denote evaluation of quantities on the boundary of P from the inside and outside respectively, and $\boldsymbol{x} = (x_1, x_2, x_3)$ in the space.

We note that χ depends linearly on $\tilde{\mathbf{e}}$ and in the sequel we indicate this by writing $\chi = \chi^{\tilde{\mathbf{e}}}$. The effective dielectric constant gives the linear map between an imposed constant electric field and the resulting average dielectric displacement seen by an observer outside the unit period cell and

is denoted by $\boldsymbol{\epsilon}_{eff} = \boldsymbol{\epsilon}_{eff}(\omega_0)$ given by

$$\boldsymbol{\epsilon}_{eff} \int_Y \boldsymbol{e}_0 \, d\boldsymbol{x} = \int_{\partial Y} \boldsymbol{x}\boldsymbol{n} \cdot \boldsymbol{e}_0 \, ds, \tag{2.7}$$

where ∂Y denotes the boundary of Y and ds is the surface area element. This formula is obtained earlier in the absence of frequency dependent dielectric inclusions in [24,31,32]. The explicit formula for $\boldsymbol{\epsilon}_{eff}$ as a function of ω_0 is given in Theorem 2.6 and constructed using generalized electrostatic resonances in Section (e).

(b) Homogenized Fields

Theorem 2.3. *(1) The plane waves (homogenized H field) $H_{hom}(\boldsymbol{x}, t)$ and the homogenized magnetic field $B_{hom}(\boldsymbol{x})$ are given by*

$$\begin{aligned} H_{hom}(\boldsymbol{x}, t) &= \left(\oint \boldsymbol{h_0} \right) e^{(ik\hat{k}\cdot\boldsymbol{x} - i\omega_0 t)}, \\ B_{hom}(\boldsymbol{x}, t) &= \mu_0 \boldsymbol{\mu}_{eff} H_{hom}(\boldsymbol{x}, t), \end{aligned} \tag{2.8}$$

where $\boldsymbol{\mu}_{eff}$ is the effective magnetic permeability tensor.

(2) The plane waves (homogenized E field) $E_{hom}(\boldsymbol{x}, t)$ and the homogenized electric displacement field $D_{hom}(\boldsymbol{x})$ are given by

$$\begin{aligned} E_{hom}(\boldsymbol{x}, t) &= \int_Y \boldsymbol{e_0} \, d\boldsymbol{x} \, e^{(ik\hat{k}\cdot\boldsymbol{x} - i\omega_0 t)}, \\ D_{hom}(\boldsymbol{x}, t) &= \epsilon_0 \boldsymbol{\epsilon}_{eff} E_{hom}(\boldsymbol{x}, t), \end{aligned} \tag{2.9}$$

where $\boldsymbol{\epsilon}_{eff}$ is the effective dielectric permittivity tensor.

The homogenized fields are the plane wave solutions of Maxwell's equations for the homogeneous effective media

$$\begin{aligned} \nabla \times E_{hom} &= -\mu_0 \boldsymbol{\mu}_{eff} \frac{\partial H_{hom}}{\partial t}, \\ \nabla \cdot D_{hom} &= 0, \\ \nabla \times H_{hom} &= \epsilon_0 \boldsymbol{\epsilon}_{eff} \frac{\partial E_{hom}}{\partial t}, \\ \nabla \cdot H_{hom} &= 0. \end{aligned} \tag{2.10}$$

The homogenized dispersion relation for the electromagnetic waves traveling through the metamaterial crystal is given by the following theorem.

Theorem 2.4. *For given $\hat{k}$ and k, the frequencies ω_0 for which plane waves can propagate with polarization $\oint \boldsymbol{h_0}$ in the direction $\hat{k}$ at wave length $\lambda = \dfrac{k}{2\pi}$ are the roots of the equation*

$$\boldsymbol{det} \left[k^2 \mathbf{A}(\omega_0) + \frac{\omega_0^2}{c^2} \boldsymbol{\mu}_{eff}(\omega_0^2) \right] = 0 \tag{2.11}$$

with $\mathbf{A}_{ij}(\omega_0) = \mathcal{E}_{ipm} \hat{k}_p \mathcal{E}_{mnj} \left[\boldsymbol{\epsilon}_{eff}^{-1}(\omega_0) \right]_{np} \hat{k}_p, \quad i, p, m, n, j = 1, 2, 3$ where $\mathcal{E}_{ipm}$ and $\mathcal{E}_{mnj}$ are the symbols for the Levi-Civita tensors.

An admissible polarization of the (homogenized H field) $H_{hom}(x, t)$ field $\oint \boldsymbol{h_0}$ lies in the null space of the matrix

$$\left[k^2 \mathbf{A}(\omega_0) + \frac{\omega_0^2}{c^2} \boldsymbol{\mu}_{eff}(\omega_0^2) \right]. \tag{2.12}$$

Using equation (2.11), we will find crystal geometries having frequency regimes where $\boldsymbol{\mu}_{eff}$ and $\boldsymbol{\epsilon}_{eff}$ are both positive, both negative or band gaps for the metamaterial.

Elimination of E_{hom} or H_{hom} from (2.10) gives

Theorem 2.5. *The homogenized fields satisfy the following vector wave equation equations for a homogeneous effective media $H_{hom}(\boldsymbol{x},t)$ satisfies*

$$\nabla\times\boldsymbol{\epsilon}_{eff}^{-1}\nabla\times H_{hom}(\boldsymbol{x},t)=-\frac{1}{c^2}\boldsymbol{\mu}_{eff}\frac{\partial^2 H_{hom}(\boldsymbol{x},t)}{\partial t^2}, \tag{2.13}$$

and $E_{hom}(\boldsymbol{x},t)$ satisfies

$$\nabla\times\boldsymbol{\mu}_{eff}^{-1}\nabla\times E_{hom}(\boldsymbol{x},t)=-\frac{1}{c^2}\boldsymbol{\epsilon}_{eff}\frac{\partial^2 E_{hom}(\boldsymbol{x},t)}{\partial t^2}. \tag{2.14}$$

(c) Effective Property Tensors as functions of frequency

Theorem 2.6. *(1) The effective magnetic permeability tensor $\boldsymbol{\mu}_{eff}$ is given by*

$$\boldsymbol{\mu}_{eff}(\omega_0)=\sum_{n=1}^{\infty}\frac{\omega_0^2/c^2}{\lambda_n\epsilon_{r,rel}^{-1}-\omega_0^2/c^2}\left(\int_Y\overline{\phi}_n\right)\otimes\left(\int_Y\phi_n\right)+\mathbf{I}^3, \tag{2.15}$$

where $\oint\phi_n=0$ and $(\lambda_n,\ \phi_n),\ n=1,2,\cdots$ are the eigenpairs of the following eigenvalue problem

$$\begin{aligned}\nabla\times\nabla\times\phi_n&=\lambda_n\phi_n \qquad in\ \ R,\\ \phi_n&=\nabla\varphi_n \qquad in\ Y\setminus R,\\ \Delta\varphi_n&=0 \qquad in\ Y\setminus R,\end{aligned} \tag{2.16}$$

with scalar potentials φ_n periodic on Y and on the boundary of R one has continuity of the normal components $\phi_n\cdot n|^-=\nabla\varphi_n\cdot n|^+$ where $|^+$ and $|^-$ denote limits from the inside and outside of the boundary of R and n is the outward directed unit normal to the boundary.
(2) The effective dielectric permittivity tensor $\boldsymbol{\epsilon}_{eff}$ is given by

$$\begin{aligned}\boldsymbol{\epsilon}_{eff}\tilde{\mathbf{e}}\cdot\tilde{\mathbf{e}}=&\big(\varepsilon_{p,rel}(\omega_0)\theta_P+\theta_M\big)\tilde{\mathbf{e}}\cdot\tilde{\mathbf{e}}\\ &+\theta_{Y\setminus R}\sum_{n=1}^{\infty}\big(1+\mu_n(\varepsilon_{p,rel}(\omega_0)-1)\big)(a_n+b_n)^2\\ &+\int_M\nabla q\cdot\nabla q+\varepsilon_{p,rel}(\omega_0)\int_P\nabla q\cdot\nabla q,\end{aligned} \tag{2.17}$$

where

$$a_n=-\tilde{\mathbf{e}}\cdot\frac{\int_M\nabla\overline{\psi}_{\mu_n}+\varepsilon_{p,rel}(\omega_0)\int_P\nabla\overline{\psi}_{\mu_n}}{1-\mu_n+\varepsilon_{p,rel}(\omega_0)\mu_n} \tag{2.18}$$

and

$$b_n=-\frac{\int_M\nabla q\cdot\nabla\overline{\psi}_{\mu_n}+\varepsilon_{p,rel}(\omega_0)\int_P\nabla q\cdot\nabla\overline{\psi}_{\mu_n}}{1-\mu_n+\varepsilon_{p,rel}(\omega_0)\mu_n}. \tag{2.19}$$

Here $\theta_P,\ \theta_M,\theta_{Y\setminus R}$ are the volumes of P, M and $Y\setminus R$ respectively, and ψ_{μ_n} are the electrostatic eigenfunctions associated to the eigenvalues $0\le\mu_n\le 1$ of the generalized electrostatic resonance eigenvalue problem [17,27]:

$$\begin{aligned}\Delta\psi_{\mu_n}&=0 \quad in\ Y\setminus R,\\ \mu_n\nabla\psi_{\mu_n}\cdot n\big|_{\partial P^+}&=(\mu_n-1)\nabla\psi_{\mu_n}\cdot n\big|_{\partial P^-},\\ \psi_{\mu_n}\big|^+_{\partial R}&=0,\end{aligned} \tag{2.20}$$

and ψ_{μ_n} is continuous in $Y\setminus R$, and satisfies periodic boundary conditions on Y. The Y-periodic continuous function q with square integrable derivatives satisfies $\Delta q=0$ in $Y\setminus R$ and $q=-\tilde{\mathbf{e}}\cdot\boldsymbol{x}$ in R.

(d) Simulation

To frame the discussion, if we assume that the material is isotropic, then for this media, the dispersion relation is given by

$$\xi_0 = \varepsilon_{r,rel} k^2 \epsilon_{eff}^{-1} \mu_{eff}^{-1} \tag{2.21}$$

where ϵ_{eff}, μ_{eff} are constants appearing in the the formulas for $\boldsymbol{\epsilon}_{eff} = \epsilon_{eff}\mathbf{I}^3$ and $\boldsymbol{\mu}_{eff} = \mu_{eff}\mathbf{I}^3$. The equation (2.21) shows the existence of ξ_0 such that both ϵ_{eff} and μ_{eff} are negative. As a demonstration, we considered cases where the metamaterial consists of unit cells in which the plasmonic coating and high dielectric core are concentric spheres located at the center of the cube as shown in FIG. 2.

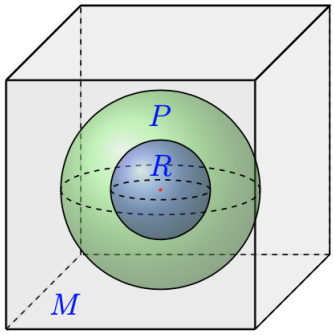

Figure 2: Unit cell with a coated spherical inclusion

In numerical computation of effective magnetic permeability, the following equivalent form of the formula (2.15) is used:

$$\boldsymbol{\mu}_{eff}(\xi_0) := \mathbf{I}_3 + \frac{1}{4}\sum_{n\in\mathbb{N}} \frac{\xi_0}{1-\alpha_n\xi_0} \left(\int_R \boldsymbol{y}\times f_n\, d\boldsymbol{y}\right) \otimes \left(\int_R \boldsymbol{y}\times f_n\, d\boldsymbol{y}\right) \tag{2.22}$$

where (α_n, f_n) are the eigenpairs of the following eigenvalue problem

$$\int_Y \nabla\Theta_f : \nabla\Theta_g\, d\boldsymbol{x} + \frac{1}{4}\left(\int_R \boldsymbol{x}\times f\, d\boldsymbol{x}\right)\cdot\left(\int_R \boldsymbol{x}\times g\, d\boldsymbol{x}\right) = \alpha\int_Y f\cdot g\, d\boldsymbol{x} \tag{2.23}$$

with g is a vector valued square integrable function such that

$$g = 0 \text{ in } Y\setminus R, \qquad \text{and} \qquad \nabla\cdot g = 0.$$

In equation (2.23), for any function h, Θ_h is constructed as follows

$$-\Delta\Theta_h = h, \text{ in } Y, \qquad \int_Y \Theta_h = 0, \tag{2.24}$$

where Θ_h is periodic. The numerical solutions of both (2.23) and (2.24) are obtained by applying FEM via FELICITY [33] in MATLAB. In order to accommodate the divergence free condition for the solution of (2.23), the solution space is discretized using the lowest order Raviart-Thomas finite elements. The solution space for (2.24) is discretized by using first order Lagrange elements.

In order to compute the effective dielectric tensor formula (2.17), we need to compute both the eigenpairs (ψ_{μ_n}, μ_n) and q. The eigenpairs (ψ_{μ_n}, μ_n) are found by solving (2.20) and the periodic function q is computed by solving the equation

$$\Delta q = 0, \qquad q\big|_{\partial R^+} = -\tilde{\boldsymbol{e}}\cdot\boldsymbol{x}. \tag{2.25}$$

Both problems (2.20) and (2.25) are solved via FELICITY [33] in MATLAB by applying FEM . The solution spaces are discretized by using first order Lagrange elements.

For the inclusions, we chose dielectric constant $\varepsilon_{r,rel} = 1$ and $\xi_p = 3 \times 10^{15}$ for the plasmon frequency of the plasmonic coating which assumed to be made of gold. We considered five different cases where the geometry is given by different radii for the concentric spherical inclusions. In the first three cases, we identified two intervals for $\xi_0/\xi_p = \omega_0^2/\omega_p^2$ where ϵ_{eff} and μ_{eff} are negative. This corresponds to the wave propagating in the direction opposite to the wave velocity. This is seen in [23] for TM transmission.

The first three cases, shown in FIG. 3, FIG. 4, and FIG. 5, demonstrate the intervals where both effective magnetic permeability and effective dielectric permittivity exhibit negative behavior. In these graphs, R and r denote the radii of the plasmonic and high dielectric inclusions respectively.

To illustrate other behaviors of effective properties, we identified two frequency intervals, shown in FIG. 6, where we observe that the effective magnetic permeability is positive while the effective dielectric permittivity remains negative. These intervals correspond to band gaps. The FIG. 7 illustrates the case of a frequency interval where both effective properties exhibit positive behavior and waves propagate along the direction of the phase velocity. In this case, we observe that the effective dielectric permittivity exhibits positive behavior when ξ_0 is close to the plasmon frequency of the gold.

By writing the formula (2.22) as

$$\boldsymbol{\mu}_{eff}\left(\frac{\omega_0^2}{\omega_p^2}\right) = \mathbf{I}_3 + \frac{1}{4}\sum_{n\in\mathbb{N}} \frac{\dfrac{\omega_0^2}{\omega_p^2}}{\dfrac{1}{\xi_p} - \alpha_n \dfrac{\omega_0^2}{\omega_p^2}} \left(\int_R \boldsymbol{y} \times f_n \, d\boldsymbol{y}\right) \otimes \left(\int_R \boldsymbol{y} \times f_n \, d\boldsymbol{y}\right), \tag{2.26}$$

it can be seen that, except for the poles of effective permeability tensor that are very close to 0, the graph of effective permeability is a horizontal line in all of the cases considered.

Figure 3 illustrates the case where the plasmonic inclusion has radius $R = 0.26$ and the high dielectric inclusion has radius $r = 0.156$. For this case we identify two frequency intervals $[0.17033, 0.171277]$ and $[0.17128, 0.17207]$ where both effective tensors are negative. Figure 4 illustrates the case where the plasmonic inclusion has radius $R = 0.3$ and the high dielectric inclusion has radius $r = 0.12$. Here we have identified two frequency intervals $[0.117425, 0.120897]$ and $[0.121006, 0.1215221]$ where both effective tensors are negative. Figure 5 illustrates the case where the plasmonic inclusion has radius $R = 0.45$ and the high dielectric inclusion has radius $r = 0.27$. For this case we identify two frequency intervals $[0.207610, 0.2105]$ and $[0.210773, 0.21203]$ where both effective tensors are negative. Figure 6 illustrates the case where the plasmonic inclusion has radius $R = 0.35$ and the high dielectric inclusion has radius $r = 0.14$. For this case we identify two frequency intervals $[0.25797, 0.259008]$ and $[0.25910, 0.26041]$ where the effective magnetic permeability is positive while the effective dielectric permittivity is negative. Figure 7 illustrates the case where the plasmonic inclusion has radius $R = 0.45$ and the high dielectric inclusion has radius $r = 0.18$. For this case we identify a frequency interval $[0.94342, 0.95728]$ where both the effective magnetic permeability tensor and the effective dielectric tensor are positive.

3. Proof of Results

(a) Leading Order Terms in Power series and Metamaterial

We carry out the analysis for the configuration shown in Figure 1, noting that a nearly identical analysis can be carried out for the coated sphere geometry with the obvious modifications. To expedite the asymptotic analysis we introduce the non-dimensional square frequency $\xi = (\varepsilon_{r,rel}\omega^2)/c^2$, square plasma frequency $\xi_p = (\omega_p^2\varepsilon_{r,rel})/c^2$, and period size $\rho = d/\sqrt{\varepsilon_{r,rel}}$, where ω_p is the plasmon frequency of the inclusion P. The non-dimensional wave number is written $\tau = \sqrt{k^2\varepsilon_{r,rel}}$.

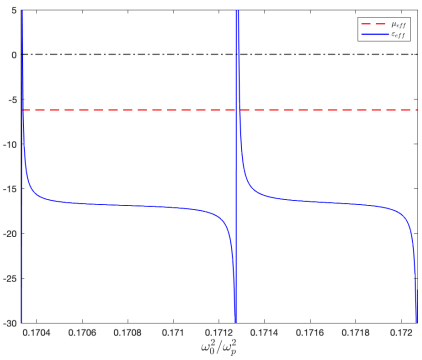

Figure 3: The case for $R = 0.26,\ r = 0.156$

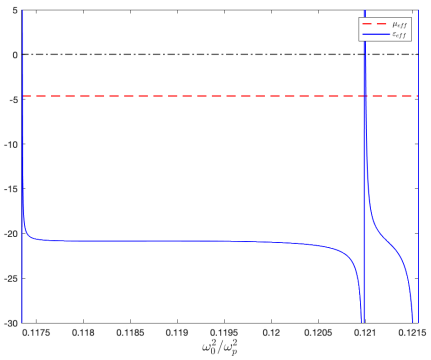

Figure 4: The case for $R = 0.3,\ r = 0.12$

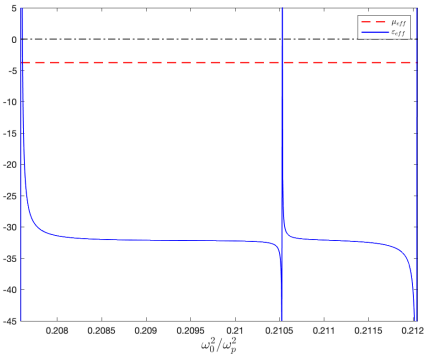

Figure 5: The case for $R = 0.45,\ r = 0.27$

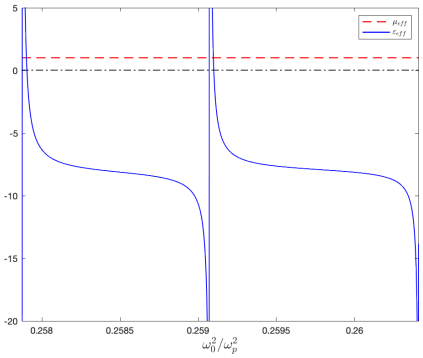

Figure 6: The case for $R = 0.35,\ r = 0.14$

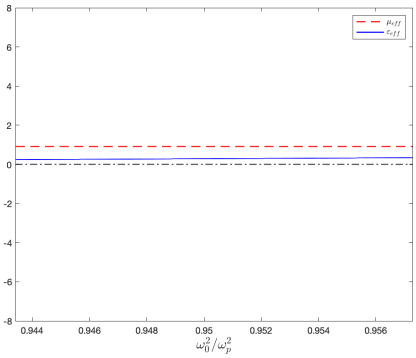

Figure 7: The case for $R = 0.45,\ r = 0.18$

We now recover the homogenization theorems. Substitution of

$$\begin{aligned}
\mathcal{E}(\boldsymbol{y}) &= \boldsymbol{e_0}(\boldsymbol{y})e^{i\eta\hat{k}\cdot\boldsymbol{y}} + \boldsymbol{e_1}(\boldsymbol{y})\eta e^{i\eta\hat{k}\cdot\boldsymbol{y}} + \boldsymbol{e_2}(\boldsymbol{y})\eta^2 e^{i\eta\hat{k}\cdot\boldsymbol{y}} + \cdots, \\
\mathcal{H}(\boldsymbol{y}) &= \boldsymbol{h_0}(\boldsymbol{y})e^{i\eta\hat{k}\cdot\boldsymbol{y}} + \boldsymbol{h_1}(\boldsymbol{y})\eta e^{i\eta\hat{k}\cdot\boldsymbol{y}} + \boldsymbol{h_2}(\boldsymbol{y})\eta^2 e^{i\eta\hat{k}\cdot\boldsymbol{y}} + \cdots, \\
\sqrt{\xi} &= \sqrt{\xi_0} + \sqrt{\xi_1}\eta + \sqrt{\xi_2}\eta^2 + \cdots
\end{aligned}$$

into (1.4) gives the following

- In R

$$\tau[(\nabla\times\boldsymbol{e_0}+i\eta\hat{k}\times\boldsymbol{e_0})+\eta(\nabla\times\boldsymbol{e_1}+i\eta\hat{k}\times\boldsymbol{e_1})+\cdots] = i\eta n_0(\sqrt{\xi_0}+\sqrt{\xi_1}\eta+\cdots)(\boldsymbol{h_0}+\eta\boldsymbol{h_1}+\cdots), \tag{3.1}$$

$$\eta[(\nabla\times\boldsymbol{h_0}+i\eta\hat{k}\times\boldsymbol{h_0})+\eta(\nabla\times\boldsymbol{h_1}+i\eta\hat{k}\times\boldsymbol{h_1})+\cdots] = -i\tau n_0^{-1}(\sqrt{\xi_0}+\sqrt{\xi_1}\eta+\cdots)(\boldsymbol{e_0}+\eta\boldsymbol{e_1}+\cdots); \tag{3.2}$$

- In P

$$\tau[(\nabla\times\boldsymbol{e_0}+i\eta\hat{k}\times\boldsymbol{e_0})+\eta(\nabla\times\boldsymbol{e_1}+i\eta\hat{k}\times\boldsymbol{e_1})+\cdots] = i\eta n_0(\sqrt{\xi_0}+\sqrt{\xi_1}\eta+\cdots)(\boldsymbol{h_0}+\eta\boldsymbol{h_1}+\cdots), \tag{3.3}$$

$$\tau[(\nabla\times\boldsymbol{h_0}+i\eta\hat{k}\times\boldsymbol{h_0})+\eta(\nabla\times\boldsymbol{h_1}+i\eta\hat{k}\times\boldsymbol{h_1})+\cdots] = -i\eta {n_0}^{-1}(\sqrt{\xi_0}+\eta\sqrt{\xi_1}+\cdots)(1-\xi^*)(\boldsymbol{e_0}+\eta\boldsymbol{e_1}+\cdots), \tag{3.4}$$

where

$$\xi^* = \frac{\xi_p}{(\sqrt{\xi_0}+\eta\sqrt{\xi_1}+\cdots)^2};$$

- In M

$$\tau[(\nabla\times\boldsymbol{e_0}+i\eta\hat{k}\times\boldsymbol{e_0})+\eta(\nabla\times\boldsymbol{e_1}+i\eta\hat{k}\times\boldsymbol{e_1})+\cdots] = i\eta n_0(\sqrt{\xi_0}+\sqrt{\xi_1}\eta+\cdots)(\boldsymbol{h_0}+\eta\boldsymbol{h_1}+\cdots), \tag{3.5}$$

$$\tau[(\nabla\times\boldsymbol{h_0}+i\eta\hat{k}\times\boldsymbol{h_0})+\eta(\nabla\times\boldsymbol{h_1}+i\eta\hat{k}\times\boldsymbol{h_1})+\cdots] = -i\eta {n_0}^{-1}(\sqrt{\xi_0}+\sqrt{\xi_1}\eta+\cdots)(\boldsymbol{e_0}+\eta\boldsymbol{e_1}+\cdots); \tag{3.6}$$

- On R-M interface

$$n\cdot(\boldsymbol{e_0}+\eta\boldsymbol{e_1}+\cdots)\big|_{\partial R^-} = \rho^2 n\cdot(\boldsymbol{e_0}+\eta\boldsymbol{e_1}+\cdots)\big|_{\partial R^+}, \tag{3.7}$$

$$n\times(\boldsymbol{e_0}+\eta\boldsymbol{e_1}+\cdots)\big|_{\partial R^-} = n\times(\boldsymbol{e_0}+\eta\boldsymbol{e_1}+\cdots)\big|_{\partial R^+}; \tag{3.8}$$

- On P-M interface

$$n\cdot\left[(\sqrt{\xi_0}+\eta\sqrt{\xi_1}+\cdots)^2-\xi_r\right](\boldsymbol{e_0}+\eta\boldsymbol{e_1}+\cdots)\big|_{\partial P^-} = n\cdot(\sqrt{\xi_0}+\eta\sqrt{\xi_1}+\cdots)^2(\boldsymbol{e_0}+\eta\boldsymbol{e_1}+\cdots)\big|_{\partial P^+}, \tag{3.9}$$

$$n\times(\boldsymbol{e_0}+\eta\boldsymbol{e_1}+\cdots)\big|_{\partial P^-} = n\times(\boldsymbol{e_0}+\eta\boldsymbol{e_1}+\cdots)\big|_{\partial P^+}. \tag{3.10}$$

We also have

- In R

$$(\nabla\cdot\boldsymbol{e_0}+i\eta\hat{k}\cdot\boldsymbol{e_0})+\eta(\nabla\cdot\boldsymbol{e_1}+i\eta\hat{k}\cdot\boldsymbol{e_1})+\cdots=0; \tag{3.11}$$

- In P

$$\varepsilon_{p,rel}[(\nabla\cdot\boldsymbol{e_0}+i\eta\hat{k}\cdot\boldsymbol{e_0})+\eta(\nabla\cdot\boldsymbol{e_1}+i\eta\hat{k}\cdot\boldsymbol{e_1})+\cdots]=0; \tag{3.12}$$

- In M

$$(\nabla\cdot\boldsymbol{e_0}+i\eta\hat{k}\cdot\boldsymbol{e_0})+\eta(\nabla\cdot\boldsymbol{e_1}+i\eta\hat{k}\cdot\boldsymbol{e_1})+\cdots=0; \tag{3.13}$$

- On R-M interface

$$n\cdot\frac{1}{\rho^2}\boldsymbol{e_i}\big|_{\partial R^-} = n\cdot\boldsymbol{e_i}\big|_{\partial R^+}; \tag{3.14}$$

- On P-M interface

$$n\cdot\varepsilon_{p,rel}\boldsymbol{e_i}\big|_{\partial P^-} = n\cdot\boldsymbol{e_i}\big|_{\partial P^+}. \tag{3.15}$$

We now collect like order terms with the same powers of η. We first recover Theorem 2.2 by collecting 0^{th} order terms in (3.1), (3.3) and (3.5), to get

$$\begin{aligned} \tau(\nabla \times \boldsymbol{e_0}) &= 0 \qquad \text{in R}, \\ \tau(\nabla \times \boldsymbol{e_0}) &= 0 \qquad \text{in P}, \\ \tau(\nabla \times \boldsymbol{e_0}) &= 0 \qquad \text{in M}. \end{aligned} \tag{3.16}$$

From (3.8), (3.10), and (3.15), we have

$$\begin{aligned} n \times \boldsymbol{e_0}\big|_{\partial R^-} &= n \times \boldsymbol{e_0}\big|_{\partial R^+}, \\ n \times \boldsymbol{e_0}\big|_{\partial P^-} &= n \times \boldsymbol{e_0}\big|_{\partial P^+}, \\ \varepsilon_{p,rel}(\omega_0) n \cdot \boldsymbol{e_0}\big|_{\partial P^-} &= n \cdot \boldsymbol{e_0}\big|_{\partial P^+}. \end{aligned} \tag{3.17}$$

From (3.11)-(3.14), we have

$$\begin{aligned} \nabla \cdot \varepsilon_{p,rel} \boldsymbol{e_0} &= 0 \qquad \text{in P}, \\ \nabla \cdot \boldsymbol{e_0} &= 0 \qquad \text{in M}, \\ \nabla \cdot \boldsymbol{e_0} &= 0 \qquad \text{in R}, \\ n \cdot \boldsymbol{e_0}\big|_{\partial R^-} &= 0. \end{aligned} \tag{3.18}$$

Using (3.16), we find

$$\int_Y |\nabla \times \boldsymbol{e_0}|^2 d\boldsymbol{y} = 0. \tag{3.19}$$

So $\nabla \times \boldsymbol{e_0} = 0$ in Y and $\boldsymbol{e_0}$ can be written as

$$\boldsymbol{e_0} = \nabla \chi^{\tilde{\mathbf{e}}} + \tilde{\mathbf{e}} \quad \text{in } Y, \tag{3.20}$$

where $\chi^{\tilde{\mathbf{e}}}$ is a Y-periodic potential with square integrable gradient and $\tilde{\mathbf{e}}$ is a complex vector. Since $\int_Y \nabla \chi^{\tilde{\mathbf{e}}} = 0$, we get that $\int_Y \boldsymbol{e_0} = \tilde{\mathbf{e}}$. Using (3.18) and (3.20), we observe that

$$\int_R |\boldsymbol{e_0}|^2 d\boldsymbol{y} = 0 \tag{3.21}$$

and this implies that $\boldsymbol{e_0} = 0$ in R and we have established Theorem 2.2.

We show that the transmission problem given by (2.5) and (2.6), follows from the asymptotic expansions. From $\boldsymbol{e_0} = \nabla \chi^{\tilde{\mathbf{e}}} + \tilde{\mathbf{e}} = 0$ in R we discover that $\chi^{\tilde{\mathbf{e}}} + \tilde{\mathbf{e}} \cdot \boldsymbol{x} = c_0$ in R, where c_0 is a constant scalar. We are free to choose the constant $c_0 = 0$ and from continuity of the potential across the boundary of R we get

$$(\chi^{\tilde{\mathbf{e}}} + \tilde{\mathbf{e}} \cdot \boldsymbol{x})\big|_{\partial R^+} = 0 \tag{3.22}$$

and (2.6) follows. The transmission problem given by (2.5) and (2.6) now follows on setting $\boldsymbol{e_0} = \nabla \chi^{\tilde{\mathbf{e}}} + \tilde{\mathbf{e}}$ and applying the last equation in (3.17) together with the first two equations in (3.18).

From linearity $\chi^{\tilde{\mathbf{e}}}$ depends linearly on $\tilde{\mathbf{e}}$ and we can write $\tilde{\mathbf{e}} = \sum_{k=1}^3 e_k \tilde{\mathbf{e}}^k$, for scalars e_k and

$$\chi^{\tilde{\mathbf{e}}} = \textstyle\sum_{k=1}^3 e_k \phi^k, \qquad k = 1, 2, 3 \tag{3.23}$$

where the potentials ϕ^k, $k = 1, 2, 3$ solve

$$\begin{aligned} &\nabla \cdot [a_p(\boldsymbol{y})(\nabla \phi^k + \tilde{\mathbf{e}}^k)] = 0 \quad \text{in } M \cup P, \\ &n \cdot \varepsilon_{p,rel}(\omega_0)(\nabla \phi^k + \tilde{\mathbf{e}}^k)\big|_{\partial P^-} = n \cdot (\nabla \phi^k + \tilde{\mathbf{e}}^k)\big|_{\partial P^+}, \end{aligned} \tag{3.24}$$

and

$$\phi^k + x_k\big|_{\partial R^+} = 0. \tag{3.25}$$

Given $\tilde{\mathbf{v}} = \sum_{k=1}^3 v_k \tilde{\mathbf{e}}^k$ set $\boldsymbol{v_0} = \nabla \chi^{\tilde{\mathbf{v}}} + \tilde{\mathbf{v}}$ where $\chi^{\tilde{\mathbf{v}}} = \sum_{k=1}^3 v_k \phi^k$. The effective bilinear form describing the effective property is defined by

$$\boldsymbol{\epsilon}_{eff} \tilde{\mathbf{e}} \cdot \tilde{\mathbf{v}} = \int_Y \varepsilon_{rel}^d (\nabla \chi^{\tilde{\mathbf{e}}} + \tilde{\mathbf{e}}) \cdot (\nabla \chi^{\tilde{\mathbf{v}}} + \tilde{\mathbf{v}})\, dy. \tag{3.26}$$

An integration by parts of (3.26) recovers the equivalent formulation of the effective dielectric constant given in (2.7).

Now, we recover Theorem 2.1. Collecting the 0^{th} order terms of η from (3.1)-(3.15) we have

$$\begin{aligned} \nabla \times \boldsymbol{h_0} &= 0 \quad \text{in } P, \\ \nabla \times \boldsymbol{h_0} &= 0 \quad \text{in } M, \\ \nabla \cdot \boldsymbol{h_0} &= 0 \quad \text{in } Y, \\ [\boldsymbol{h_0}] &= 0 \quad \text{on } \partial P \text{ and } \partial R. \end{aligned} \tag{3.27}$$

Finally, we write (3.2) as

$$(\nabla + i\eta\hat{k}) \times (\boldsymbol{h_0} + \eta \boldsymbol{h_1} + \cdots) = -i\frac{n_0^{-1}}{\rho}(\sqrt{\xi_0} + \eta\sqrt{\xi_1} + \cdots)(\boldsymbol{e_0} + \eta \boldsymbol{e_1} + \cdots). \tag{3.28}$$

By applying the differential operator $(\nabla + i\eta\hat{k})\times$ to the both side of (3.28) and collecting the 0^{th} order and first order terms of η, we find that

$$\nabla \times \nabla \times \boldsymbol{h_0} = \xi_0 \boldsymbol{h_0} \qquad \text{in} \quad R. \tag{3.29}$$

Since $\boldsymbol{h}_0$ is divergence free on Y and $\nabla \times \boldsymbol{h}_0 = 0$ on $Y \setminus R$, there is a potential w and a constant vector $\mathbf{c}$ such that $\boldsymbol{h}_0 = \nabla w + \mathbf{c}$ on $Y \setminus R$ with $\Delta w = 0$ there and periodic on the boundary of Y. Theorem 2.1 now follows.

To see Theorem 2.1 note that since $\boldsymbol{h}_0 = \nabla w + \mathbf{c}$, where w is periodic on the boundary of Y, then direct calculation shows $\oint \boldsymbol{h}_0 = \mathbf{c}$ for any choice of Γ_k, $k = 1.2.3$.

(b) Derivation of Homogenized Fields

We focus now on recovering the homogenized equations (2.10) from the expansions. We collect terms of the first order in η in (3.1), (3.3) and (3.5), and get

$$\begin{aligned} \tau(\nabla \times \boldsymbol{e_1}) &= i\sqrt{\xi_0} n_0 h_0 \qquad \text{in R}, \\ \tau(\nabla \times \boldsymbol{e_1} + i\hat{k} \times \boldsymbol{e_0}) &= i\sqrt{\xi_0} n_0 h_0 \qquad \text{in P}, \\ \tau(\nabla \times \boldsymbol{e_1} + i\hat{k} \times \boldsymbol{e_0}) &= i\sqrt{\xi_0} n_0 h_0 \qquad \text{in M}. \end{aligned} \tag{3.30}$$

Integrate the equations in (3.30) over the regions R, P and M, respectively. The summation of these three integrals gives

$$\tau \int_Y i\hat{k} \times \boldsymbol{e_0}\, d\boldsymbol{y} = i n_0 \sqrt{\xi_0} \int_Y \boldsymbol{h_0}\, d\boldsymbol{y}. \tag{3.31}$$

Collecting terms of second order in η in (3.2) and first order in η in (3.4) and (3.6) gives

$$\begin{aligned} \nabla \times \boldsymbol{h_1} + i\hat{k} \times \boldsymbol{h_0} &= -i\tau n_0^{-1}(\sqrt{\xi_1}\boldsymbol{e_1} + \sqrt{\xi_0}\boldsymbol{e_2}) \quad \text{in R}, \\ \tau(\nabla \times \boldsymbol{h_1} + i\hat{k} \times \boldsymbol{h_0}) &= -i\varepsilon_{p,rel}(\xi_0)\sqrt{\xi_0} n_0^{-1} \boldsymbol{e_0} \quad \text{in P}, \\ \tau(\nabla \times \boldsymbol{h_1} + i\hat{k} \times \boldsymbol{h_0}) &= -i\sqrt{\xi_0} n_0^{-1} \boldsymbol{e_0} \qquad \text{in M}. \end{aligned} \tag{3.32}$$

On setting $\boldsymbol{e^{*,i}} = \nabla\phi^i + \tilde{\mathbf{e}}^i$, $i = 1, 2, 3$, we have

$$\boldsymbol{e^{*,i}} = 0 \ \text{ in R}, \quad \nabla \cdot \boldsymbol{e^{*,i}} = 0 \ \text{ in Y}, \quad \text{and} \quad \int_Y \boldsymbol{e^{*,i}} = \tilde{\mathbf{e}}^i, \ \ i = 1, 2, 3. \tag{3.33}$$

We multiply the equations in (3.32) by $\boldsymbol{e}^{*,\boldsymbol{i}}$ and then integrate them over the regions R, P and M, respectively. Adding the integrals together gives

$$\begin{aligned}&\tau\left(\int_Y \nabla\times\boldsymbol{h_1}\cdot\boldsymbol{e}^{*,\boldsymbol{i}}\,d\boldsymbol{y}+\int_Y i\hat{k}\times\boldsymbol{h_0}\cdot\boldsymbol{e}^{*,\boldsymbol{i}}\,d\boldsymbol{y}\right)\\&=-in_0^{-1}\sqrt{\xi_0}\int_Y \varepsilon^d_{rel}(\xi_0,\boldsymbol{y})\boldsymbol{e_0}\cdot\boldsymbol{e}^{*,\boldsymbol{i}}\,d\boldsymbol{y}.\end{aligned}\tag{3.34}$$

Applying the definition of the effective magnetic permeability (2.2) to the equation (3.31) we obtain

$$\tau\,\hat{k}\times\left(\int_Y \boldsymbol{e_0}\right)=n_0\sqrt{\xi_0}\boldsymbol{\mu}_{eff}\left(\oint \boldsymbol{h_0}\right).\tag{3.35}$$

Note that $\nabla\times\boldsymbol{e_0}=0$ in Y implies $\nabla\times\boldsymbol{e}^{*,\boldsymbol{i}}=0$ in Y. So we can show $\nabla\cdot(\boldsymbol{e}^{*,\boldsymbol{i}}\times k)=0$. Therefore, an application of Lemma 4.5 of [24] to the second term of the left hand hand side of (3.34) gives

$$\begin{aligned}i\tau\int_Y \hat{k}\times\boldsymbol{h_0}\cdot\boldsymbol{e}^{*,\boldsymbol{i}}\,d\boldsymbol{y}&=i\tau\int_Y \boldsymbol{h_0}\cdot(\hat{k}\times\boldsymbol{e}^{*,\boldsymbol{i}})\\&=i\tau\left(\hat{k}\times\oint\boldsymbol{h_0}\right)\cdot\tilde{\mathbf{e}}^{i}.\end{aligned}\tag{3.36}$$

A direct calculation gives

$$\int_Y \nabla\times\boldsymbol{h_1}\cdot\boldsymbol{e}^{*,\boldsymbol{i}}=0.\tag{3.37}$$

Finally, applying (3.37) and (3.36) in (3.34) gives

$$i\tau\left(\hat{k}\times\oint\boldsymbol{h_0}\right)\cdot\tilde{\mathbf{e}}^{i}=-in_0^{-1}\sqrt{\xi_0}\int_Y \varepsilon^d_{rel}(\xi_0,\boldsymbol{y})(\nabla\chi^{\tilde{\mathbf{e}}}+\tilde{\mathbf{e}})\cdot\mathbf{e}^{*,i}\,d\boldsymbol{y}.\tag{3.38}$$

From linearity we express the effective dielectric permittivity tensor $\boldsymbol{\epsilon}_{eff}$ as

$$[\boldsymbol{\epsilon}_{eff}]_{ij}:=\int_Y \varepsilon^d_{rel}(\xi_0,\boldsymbol{y})\mathbf{e}^{*,i}\cdot\mathbf{e}^{*,j}\,d\boldsymbol{y},\tag{3.39}$$

and (3.38) and (3.39) give

$$\int_Y \boldsymbol{e_0}\,d\boldsymbol{y}=-\tau\frac{n_0}{\sqrt{\xi_0}}\boldsymbol{\epsilon}^{-1}_{eff}\left(\hat{k}\times\oint\boldsymbol{h_0}\right).\tag{3.40}$$

Substituting (3.40) into (3.35) gives

$$-\tau^2\hat{k}\times\boldsymbol{\epsilon}^{-1}_{eff}\hat{k}\times\oint\boldsymbol{h_0}=\xi_0\boldsymbol{\mu}_{eff}\oint\boldsymbol{h_0},\tag{3.41}$$

which then yields

$$\nabla_{\boldsymbol{x}}\times\boldsymbol{\epsilon}^{-1}_{eff}\nabla_{\boldsymbol{x}}\times\oint\boldsymbol{h_0}\,e^{ik\hat{k}\cdot\boldsymbol{x}}=\frac{\omega_0^2}{c^2}\boldsymbol{\mu}_{eff}\oint\boldsymbol{h_0}\,e^{ik\hat{k}\cdot\boldsymbol{x}}.\tag{3.42}$$

Multiplying $e^{-i\omega_0 t}$ to the both sides of (3.42) and noting that $H_{\text{hom}}(\boldsymbol{x},t)=\left(\oint\boldsymbol{h_0}\right)e^{(ik\hat{k}\cdot\boldsymbol{x}-i\omega_0 t)}$ completes the proof of (2.13).

By expressing $\oint\boldsymbol{h}_0$ in (3.35) and using (3.38), we get

$$\nabla_{\boldsymbol{x}}\times\boldsymbol{\mu}^{-1}_{eff}\times\int_Y \boldsymbol{e_0}\,e^{ik\hat{k}\cdot\boldsymbol{x}}=\frac{\omega_0^2}{c^2}\boldsymbol{\varepsilon}_{eff}\int_Y \boldsymbol{e_0}\,e^{ik\hat{k}\cdot\boldsymbol{x}}.$$

Multiplying $e^{-i\omega_0 t}$ to the both sides and noting that $E_{\text{hom}}(\boldsymbol{x},t)=\int_Y \boldsymbol{e_0}\;d\boldsymbol{x}\;e^{(ik\hat{k}\cdot\boldsymbol{x}-i\omega_0 t)}$ completes the proof of (2.14).

(c) Derivation of Maxwell's System for Homogenized Fields

Using equations (3.35), (3.40), and $n_0 = \sqrt{\mu_0/\varepsilon_0}$, $c = \dfrac{1}{\sqrt{\mu_0\varepsilon_0^2}}$, $\sqrt{\xi_0} = \dfrac{\omega_0}{c}\sqrt{\varepsilon_{r,rel}}$, we find

$$\nabla_{\boldsymbol{x}} \times \left(\int_Y \boldsymbol{e}_0 \, e^{ik\hat{k}\cdot\boldsymbol{x}} \right) = i\varepsilon_0\omega_0 \boldsymbol{\mu}_{eff} \left(\oint \boldsymbol{h}_0 \, e^{ik\hat{k}\cdot\boldsymbol{x}} \right),$$

$$\nabla_{\boldsymbol{x}} \times \left(\oint_Y \boldsymbol{h}_0 \, e^{ik\hat{k}\cdot\boldsymbol{x}} \right) = -i\mu_0\omega_0 \boldsymbol{\varepsilon}_{eff} \left(\int \boldsymbol{e}_0 \, e^{ik\hat{k}\cdot\boldsymbol{x}} \right).$$

Finally, multiplying $e^{-i\omega_0 t}$ to both sides of the above equations and using (2.8) and (2.9) complete the proof of the first and the third equations in (2.10). The second and the fourth equations of (2.10) are the direct consequence of applying the divergence operator to H_{hom} and E_{hom} in (2.8) and (2.9).

(d) Demonstration of Dispersion Relation

Using Einstein summation notation and Levi-Civita tensor notations, we have

$$\xi_0 \boldsymbol{\mu}_{eff}(\xi_0) \oint \boldsymbol{h}_0 = \xi_0 \left[\boldsymbol{\mu}_{eff}(\xi_0)\right]_{ij} \left[\oint \boldsymbol{h}_0\right]_j, \tag{3.43}$$

$$\left(\hat{k} \times \left[\boldsymbol{\varepsilon}_{eff}^{-1}(\xi_0)\hat{k} \times \oint \boldsymbol{h}_0\right] \right)_i = \mathcal{E}_{ipm}\hat{k}_p\mathcal{E}_{mnj} \left[\boldsymbol{\varepsilon}_{eff}^{-1}(\xi_0)\right]_{np} \hat{k}_p \left[\oint \boldsymbol{h}_0\right]_j, \tag{3.44}$$

where $i, p, m, n, j = 1, 2, 3$. So equation (3.41) is written by components as

$$\begin{aligned} 0 &= \tau^2 \, \hat{k} \times \boldsymbol{\varepsilon}_{eff}^{-1}(\xi_0)\hat{k} \times \oint \boldsymbol{h}_0 + \xi_0 \boldsymbol{\mu}_{eff}(\xi_0) \oint \boldsymbol{h}_0 \\ &= \tau^2 \mathcal{E}_{ipm}\hat{k}_p\mathcal{E}_{mnj} \left[\boldsymbol{\varepsilon}_{eff}^{-1}(\xi_0)\right]_{np} \hat{k}_p \left[\oint \boldsymbol{h}_0\right]_j + \xi_0 \left[\boldsymbol{\mu}_{eff}(\xi_0)\right]_{ij} \left[\oint \boldsymbol{h}_0\right]_j. \end{aligned} \tag{3.45}$$

Equation (3.45) implies that the determinant equation for ξ_0 at a given wave number k can be written as

$$\begin{aligned} &\mathbf{det}\left[\tau^2 \mathbf{A} + \xi_0 \boldsymbol{\mu}_{eff}(\xi_0)\right] = 0, \\ &\mathbf{A}_{ij} = \mathcal{E}_{ipm}\hat{k}_p\mathcal{E}_{mnj} \left[\boldsymbol{\varepsilon}_{eff}^{-1}(\xi_0)\right]_{np} \hat{k}_p, \end{aligned} \tag{3.46}$$

where $i, p, m, n, j = 1, 2, 3$. Noting that $\tau^2 = k^2\varepsilon_{r,rel}, \xi_0 = \dfrac{\omega_0^2}{c^2}\varepsilon_{r,rel}$ completes the proof.

(e) Effective Property Tensors and Their Meaning as Explicit Functions of ξ_0

The effective permittivity (2.2) and its formula (2.15) follows from an eigenfunction expansion of $\boldsymbol{h_0}$. Here we use the eignfunctions given in Theorem 2.6. These eigenfunctions form an complete orthonormal system with respect to the inner product $(\boldsymbol{h}, \boldsymbol{w}) := \int_Y \boldsymbol{h} \cdot \overline{\boldsymbol{w}} \, dy$, i.e., $(\phi_i, \phi_j) = \delta_{ij}$. It is easily seen as in [24] that $\boldsymbol{h}_0 - \fint \boldsymbol{h}_0$ lies in the span of $\{\phi_n\}$ and we write $\boldsymbol{h}_0 = \sum_{j=1}^{\infty} c_j\phi_j + \mathbf{c}$, where $\mathbf{c} = \fint \boldsymbol{h}_0$ and determine the coefficients c_j. Substitution into (2.1) gives

$$c_j = \frac{\xi_0 \, \mathbf{c} \cdot \int_Y \overline{\phi}_j}{\lambda_i - \xi_0}. \tag{3.47}$$

So

$$\boldsymbol{h}_0 = \sum_{j=1}^{\infty} \frac{\xi_0 \, \mathbf{c} \cdot \int_Y \overline{\phi}_j \, d\boldsymbol{x}}{\lambda_i - \xi_0} \phi_j + \mathbf{c}. \tag{3.48}$$

Hence

$$\int_y \boldsymbol{h}_0\, d\boldsymbol{x} = \sum_{j=1}^{\infty} \frac{\xi_0\, \mathbf{c}\cdot\int_Y \overline{\phi}_j\, d\boldsymbol{x}}{\lambda_j-\xi_0}\int_Y \phi_j\, d\boldsymbol{x} + \mathbf{c} \tag{3.49}$$

$$= \left(\sum_{j=1}^{\infty} \frac{\xi_0}{\lambda_j-\xi_0}\int_Y \overline{\phi}_j\, d\boldsymbol{x}\otimes\int_Y \phi_j\, d\boldsymbol{x} + I\right)\oint \boldsymbol{h}_0 \tag{3.50}$$

$$= \tilde{\boldsymbol{\mu}}_{eff}(\xi_0)\oint \boldsymbol{h}_0, \tag{3.51}$$

and the formula for $\boldsymbol{\mu}_{eff}(\omega_0)$ follows noting that $\boldsymbol{\mu}_{eff}(\omega_0) = \tilde{\boldsymbol{\mu}}_{eff}(\xi_0)$.

Formula (2.17) follows from an eigenfunction expansion of $\chi^{\tilde{\mathbf{e}}}$. Here we use the eignfunctions given by (2.20). The set of these functions form a complete orthonormal set over the space of continuous functions periodic in Y with zero average and square integrable gradient that are zero in R, with inner product $\langle\psi,\phi\rangle = \int_{Y/R}\nabla\psi\cdot\nabla\overline{\phi}\,dx$.

Let

$$\chi^{\tilde{\mathbf{e}}} = w + r + q, \tag{3.52}$$

where w satisfies

$$\nabla\cdot\left(\varepsilon^d_{rel}(\omega_0)(\nabla w+\tilde{\mathbf{e}})\right) = 0 \text{ in } Y\setminus R; \tag{3.53}$$

r satisfies

$$\nabla\cdot\left(\varepsilon^d_{rel}(\omega_0)(\nabla r+\nabla q)\right) = 0 \text{ in } Y\setminus R; \tag{3.54}$$

and q satisfies $\Delta q = 0$ in $Y\setminus R$ and $q = -\tilde{\mathbf{e}}\cdot x$ in R. The functions w and r admit the eigenfunction expansion

$$w = \sum_{n=1}^{\infty} a_n\psi_{\mu_n} \text{ and } r = \sum_{n=1}^{\infty} b_n\psi_{\mu_n}. \tag{3.55}$$

Multiplying (3.53) by $\nabla\overline{\psi}_{\mu_n}$, integrating over $Y\setminus R$, and using the jump condition $n\cdot\varepsilon_{p,rel}(\omega_0)(\nabla w+\tilde{\mathbf{e}})\big|_{\partial P^-} = n\cdot(\nabla w+\tilde{\mathbf{e}})\big|_{\partial P^+}$, we deduce that

$$a_n = -\tilde{\mathbf{e}}\cdot\frac{\int_M \nabla\overline{\psi}_{\mu_n} + \varepsilon_{p,rel}(\omega_0)\int_P \nabla\overline{\psi}_{\mu_n}}{1-\mu_n+\varepsilon_{p,rel}(\omega_0)\mu_n}. \tag{3.56}$$

In a similar way, from (3.54) we deduce that

$$b_n = -\frac{\int_M \nabla q\cdot\nabla\overline{\psi}_{\mu_n} + \varepsilon_{p,rel}(\omega_0)\int_P \nabla q\cdot\nabla\overline{\psi}_{\mu_n}}{1-\mu_n+\varepsilon_{p,rel}(\omega_0)\mu_n}. \tag{3.57}$$

Using the orthogonality and substituting (3.52) and (3.55) – (3.57) into (3.26) with $\tilde{\mathbf{v}} = \tilde{\mathbf{e}}$, we obtain

$$\begin{aligned}\boldsymbol{\epsilon}_{eff}\tilde{\mathbf{e}}\cdot\tilde{\mathbf{e}} = &\left(\varepsilon_{p,rel}(\omega_0)\theta_P+\theta_M\right)\tilde{\mathbf{e}}\cdot\tilde{\mathbf{e}}\\ &+\theta_{Y\setminus R}\sum_{n=1}^{\infty}\left(1+\mu_n(\varepsilon_{p,rel}-1)\right)(a_n+b_n)^2\\ &+\int_M \nabla q\cdot\nabla q + \varepsilon_{p,rel}\int_P \nabla q\cdot\nabla q.\end{aligned} \tag{3.58}$$

And the proof of Theorem 2.6 (2) is concluded.

4. Conclusion

The frequency dependent effective dielectric permittivity and magnetic permeability are described by two types of subwavelength resonances: a plasmon resonance generating frequency

dependent positive or negative effective dielectric properties and an artificial magnetic resonance generating a frequency dependent effective magnetic permeability. In this article we show how to employ these two resonances to rationally design double negative metamaterials. We numerically calculate the effective properties for metamaterial crystals made from coated sphere geometries and identified frequency intervals in the near infrared-optical regime where the metamaterial exhibits double negative behavior. The term double negative refers to simultaneously negative effective magnetic permeability and dielectric permittivity, implying that the propagation of energy is opposite to the direction of phase velocity. The dependence of the sign of the effective magnetic permeability and effective dielectric permittivity depends on frequency. Frequency intervals corresponding to band gaps as well as intervals of normal dispersion and double negative dispersion are controlled explicitly through the geometry as seen in the theory and numerical experiments. Here phenomenological modeling is not used but instead all results follow directly the Maxwell system on substituting a power series representation of the solution and examining leading order behavior. We expect similar rigorous arguments to show that the power series represents the solution in 3 dimensions and this is a project for future work.

Data Accessibility. Source code and files of all computations have been made available at https://github.com/Adil-Abit/Controlling-the-Dispersion-of-Metamaterials-in-3-d.

Authors' Contributions. A.A.,Y.C. and R.L. contributed to the conception and analysis of the mathematical method. A.A. and S.W. developed the code, S.W. developed numerical method. A.A., Y.C. and R.L. designed the numerical tests. A.A. performed the numerical simulation. All authors critically discussed the numerical results. All authors contributed to writing and editing the paper. All authors gave final approval for publication.

Competing Interests. We have no competing interests.

Funding. This research work is supported in part by NSF Grants DMS-1813698, DMREF-1921707.

References

1. Viktor G Veselago. Electrodynamics of substances with simultaneously negative values of ϵ and μ. *Usp. Fiz. Nauk*, 92:517, 1967.
2. John B Pendry, Anthony J Holden, David J Robbins, and WJ Stewart. Magnetism from conductors and enhanced nonlinear phenomena. *IEEE transactions on microwave theory and techniques*, 47(11):2075–2084, 1999.
3. David R Smith, Willie J Padilla, DC Vier, Syrus C Nemat-Nasser, and Seldon Schultz. Composite medium with simultaneously negative permeability and permittivity. *Physical review letters*, 84(18):4184, 2000.
4. Fuli Zhang, Sylvain Potet, Jorge Carbonell, Eric Lheurette, Olivier Vanbesien, Xiaopeng Zhao, and Didier Lippens. Negative-zero-positive refractive index in a prism-like omega-type metamaterial. *IEEE transactions on microwave theory and techniques*, 56(11):2566–2573, 2008.
5. Shuang Zhang, Wenjun Fan, BK Minhas, Andrew Frauenglass, KJ Malloy, and SRJ Brueck. Midinfrared resonant magnetic nanostructures exhibiting a negative permeability. *Physical review letters*, 94(3):037402, 2005.
6. Xin Zhou and XP Zhao. Resonant condition of unitary dendritic structure with overlapping negative permittivity and permeability. *Applied Physics Letters*, 91(18):181908, 2007.
7. Jiangtao Huangfu, Lixin Ran, Hongsheng Chen, Xian-min Zhang, Kangsheng Chen, Tomasz M Grzegorczyk, and Jin Au Kong. Experimental confirmation of negative refractive index of a metamaterial composed of ω-like metallic patterns. *Applied Physics Letters*, 84(9):1537–1539, 2004.
8. Gunnar Dolling, Christian Enkrich, Martin Wegener, Costas M Soukoulis, and Stefan Linden. Low-loss negative-index metamaterial at telecommunication wavelengths. *Optics letters*, 31(12):1800–1802, 2006.
9. Vladimir M Shalaev, Wenshan Cai, Uday K Chettiar, Hsiao-Kuan Yuan, Andrey K Sarychev, Vladimir P Drachev, and Alexander V Kildishev. Negative index of refraction in optical metamaterials. *Optics letters*, 30(24):3356–3358, 2005.
10. Kerwyn Casey Huang, ML Povinelli, and John D Joannopoulos. Negative effective permeability in polaritonic photonic crystals. *Applied Physics Letters*, 85(4):543–545, 2004.

11. Liang Peng, Lixin Ran, Hongsheng Chen, Haifei Zhang, Jin Au Kong, and Tomasz M Grzegorczyk. Experimental observation of left-handed behavior in an array of standard dielectric resonators. *Physical review letters*, 98(15):157403, 2007.
12. Kevin Vynck, Didier Felbacq, Emmanuel Centeno, AI Căbuz, David Cassagne, and Brahim Guizal. All-dielectric rod-type metamaterials at optical frequencies. *Physical review letters*, 102(13):133901, 2009.
13. Mark S Wheeler, J Stewart Aitchison, and Mohammad Mojahedi. Coated nonmagnetic spheres with a negative index of refraction at infrared frequencies. *Physical Review B*, 73(4):045105, 2006.
14. Vassilios Yannopapas. Artificial magnetism and negative refractive index in three-dimensional metamaterials of spherical particles at near-infrared and visible frequencies. *Applied Physics A*, 87(2):259–264, 2007.
15. Vassilios Yannopapas. Negative refractive index in the near-uv from au-coated cucl nanoparticle superlattices. *physica status solidi (RRL)–Rapid Research Letters*, 1(5):208–210, 2007.
16. Yue Chen and Robert Lipton. Multiscale methods for engineering double negative metamaterials. *Photonics and Nanostructures-Fundamentals and Applications*, 11(4):442–452, 2013.
17. Yue Chen and Robert Lipton. Resonance and double negative behavior in metamaterials. *Archive for Rational Mechanics and Analysis*, 209(3):835–868, 2013.
18. Gennady Shvets and Yaroslav A Urzhumov. Engineering the electromagnetic properties of periodic nanostructures using electrostatic resonances. *Physical review letters*, 93(24):243902, 2004.
19. Andrea Alù and Nader Engheta. Dynamical theory of artificial optical magnetism produced by rings of plasmonic nanoparticles. *Physical Review B*, 78(8):085112, 2008.
20. Santiago P Fortes, Robert P Lipton, and Stephen P Shipman. Sub-wavelength plasmonic crystals: dispersion relations and effective properties. *Proceedings of the Royal Society A: Mathematical, Physical and Engineering Sciences*, 466(2119):1993–2020, 2010.
21. Santiago P Fortes, Robert P Lipton, and Stephen P Shipman. Convergent power series for fields in positive or negative high-contrast periodic media. *Communications in Partial Differential Equations*, 36(6):1016–1043, 2011.
22. Stephen P Shipman. Power series for waves in micro-resonator arrays. In *2010 International Conference on Mathematical Methods in Electromagnetic Theory*, pages 1–6. IEEE, 2010.
23. Yue Chen and Robert Lipton. Controlling refraction using sub-wavelength resonators. *Applied Sciences*, 8(10):1942, 2018.
24. Guy Bouchitté, Christophe Bourel, and Didier Felbacq. Homogenization near resonances and artificial magnetism in three dimensional dielectric metamaterials. *Archive for Rational Mechanics and Analysis*, 225(3):1233–1277, 2017.
25. Robert Lipton and Ben Schweizer. Effective maxwell's equations for perfectly conducting split ring resonators. *Archive for Rational Mechanics and Analysis*, 229(3):1197–1221, 2018.
26. Agnes Lamacz and Ben Schweizer. A negative index meta-material for maxwell's equations. *SIAM Journal on Mathematical Analysis*, 48(6):4155–4174, 2016.
27. Robert Lipton, Robert Viator, Jiminez Bolanos, and Abiti Adili. Bloch waves in high contrast electromagnetic crystals. *ArXive for Math*, Arxiv:2110.12262v1, 2021.
28. D.J. Bergman. The dielectric constant of a composite material - a problem in classical physics. *Physics Reports*, 43:377–407, 1978.
29. R.C. McPhedran and G.W. Milton. Bounds and exact theories for transport properties of inhomogeneous media. *Applied Physics A.*, 26:207–220, 1981.
30. I. Mayergoyz, D. Fredkin, and Z. Zhang. Electrostatic (plasmon) resonances in nanoparticles. *Physical Review B*, 72, 2005.
31. Klaas Hendrik Poelstra, Ben Schweizer, and Maik Urban. The geometric average of curl-free fields in periodic geometries. *Analysis*, 41(3):179–197, 2021.
32. Guy Bouchitté and Ben Schweizer. Homogenization of maxwell's equations in a split ring geometry. *Multiscale Modeling & Simulation*, 8(3):717–750, 2010.
33. Shawn W Walker. Felicity: A matlab/c++ toolbox for developing finite element methods and simulation modeling. *SIAM Journal on Scientific Computing*, 40(2):C234–C257, 2018.